

Behavior and design of fastenings with headed anchors at the edge under tension and shear load

J. Hofmann, R. Eligehausen & J. Ožbolt

Institute of Construction Materials, University of Stuttgart, Germany

ABSTRACT: In the present paper the theoretical aspects and the application of the non-linear finite element program MASA for analysis of anchorages placed at an edge of a concrete block are discussed. After an introduction the structure of the finite element (FE) code is briefly described. The results of the simulations are shown and compared with experimental data. They confirm that the FE code is able to simulate realistically the behavior of anchorages. Subsequently a parametric study is carried out and the results are discussed.

1 INTRODUCTION

The failure load of anchorages with headed studs may be calculated according to the CC – method by Fuchs, Eligehausen, Breen (1995). In order to understand the behavior of headed studs very close to an edge under tension and shear loading in more detail and possibly to improve the CC – method, a numerical investigation was carried out with the non-linear FE code MASA. It is based on the microplane model. The program is able to analyze the three-dimensional nonlinear behavior of concrete.

In the present paper it is shown that the program MASA is able to predict realistically the behavior of fastenings with headed anchors close to an edge. Furthermore the influence of the most important concrete properties and geometrical parameters on the failure load is shown.

2 FINITE-ELEMENT-CODE MASA

2.1 General

The used finite element code is based on the microplane model. It can be used for the two and the three-dimensional analysis of quasi brittle materials. The model allows a realistic prediction of the material behavior in case of three-dimensional stress - strain states. The smeared crack approach is employed. To ensure a mesh independent crack development a so-called "localization limiter" is used. This is realized by the crack band approach or by a generalized nonlocal integral method. For the analyses discussed in the present paper, the improved crack band approach was used. The material model is described in detail in Ožbolt et al. (2001)

The concrete is discretized by 8-node brick elements. The reinforcing bars are modeled with bar elements or smeared within the concrete elements. Beside the standard finite elements special contact elements are available. They allow a simulation of the contact between concrete and headed stud. The analysis is incremental. For simple handling of the program as well as for the pre and post processing the commercial program FEMAP (1997) is used.

2.2 Constitutive law – Microplane model

In the microplane model the material properties are characterized separately on planes of various orientations within the material. On these microplanes there are only a few uniaxial stress and strain components and no tensorial invariance requirements need to be considered. The constitutive properties are entirely characterized by relations between the stress and strain components on each microplane in both, normal and shear directions (Fig. 1). It is assumed that the strain components on the microplanes are projections of the macroscopic strain tensor (kinematic constraint approach). Knowing the stress-strain relationship of all microplane components, the macroscopic stiffness and the stress tensor are calculated from the actual strains on the microplanes by integrating the stress components on the microplanes over all directions. The simplicity of the model is due to the fact that only uniaxial stress-strain relationships are required for each microplane component and the macroscopic response is obtained automatically by integration over the microplanes. More details related to the used model can be found in Ožbolt et al. (2001).

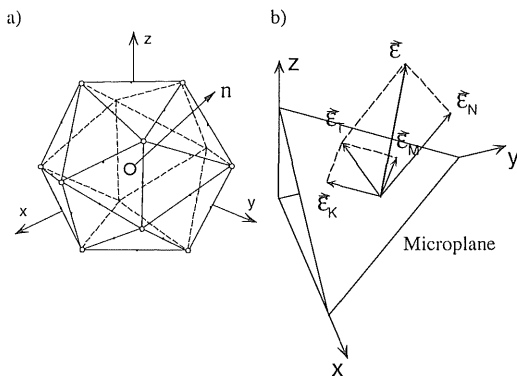


Figure 1. Concept of the microplane model: a) unit volume sphere – integration point and b) strain components.

3 COMPARISON BETWEEN TEST DATA AND NUMERICAL ANALYSIS IN CASE OF BLOW OUT FAILURE

To verify the suitability of the finite element program MASA for the numerical simulation of headed studs placed close to the edge of a concrete block a numerical study was carried out and the results are compared with experimental results.

3.1 Geometry and discretization

The geometry of the modeled anchorage structure is shown in Figure 2a. A concrete slab with a width of $b = c + 400$ mm ($c =$ concrete cover), a length of 800 mm and a height of 380 mm is analyzed. The material properties are adapted to the properties known from the experiments and are summarized in Table 1.

Figure 2 also shows the finite element mesh used in the analysis. The existing symmetry plane was used to reduce the analysis time. The mesh was refined within the area of the headed stud. The modeled test specimen is restrained in vertical direction at a distance of 85 mm from the anchor (Fig. 2b). The numerical analysis considers the same boundary conditions as in the experiment (Furche, Eligehausen 1991).

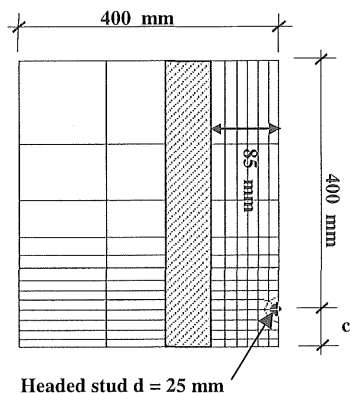
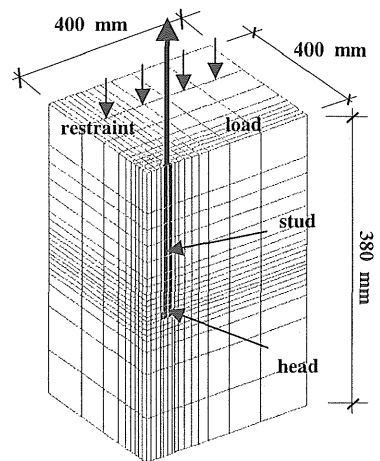
The discretization of the concrete slab was performed by eight - node solid elements. The microplane model was used. Linear elastic material behavior was assumed for steel elements.

Between the steel elements of the headed stud and the concrete elements contact elements were placed. These elements have a thickness of 0.5 mm. They were chosen such that only compressive stresses between concrete and anchor could be taken up.

The load was applied by displacement control at the nodes of the headed stud. The displacement was increased by 0.05 mm in each step.

Table 1 : Material properties assumed in the analysis.

concrete				geometry				steel	
G_f	f_{ctm}	E_{beton}	β_w	h_{ef}	a	γ	c	E_{S1ahl}	f_y
[Mpa]	[Mpa]	[Mpa]	[Mpa]	[mm]	[mm]	[°]	[mm]	[Mpa]	[Mpa]
0,075	2,5	35000	35	400	7,5	90	60	20000	2000



a)

b)

Figure 2. Dimensions of the FE – model.

3.2 Numerical results and comparison with test results

In both the experimental and the numerical investigations a characteristic blow out failure could be ob-

served. The damage zone obtained in the analysis is shown in Figure 3 as maximum principal strains. The dark areas are the areas of strain localization (damage). The comparison shows a good agreement between the failure mode observed in the experiments and the analysis.

The displacements and the anchor forces were taken at the head of the stud. At maximum load the displacement measured in the experiment is slightly larger than in the simulation. This is due to the complex conditions when local damage at the head of the stud takes place.

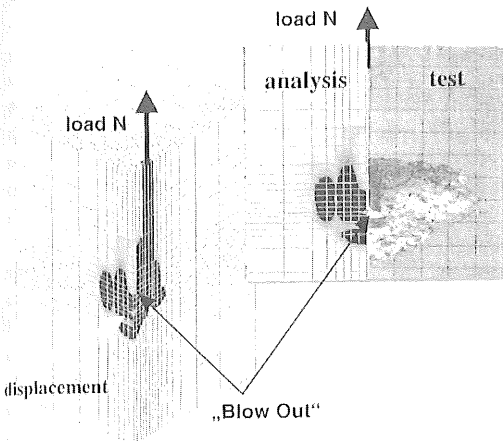


Figure 3. Post peak crack pattern, $h_{ef} = 400$ mm (embedment depth), $c = 60$ mm (edge distance), $a = 7,5$ mm (head shoulder). Experiment by Furche, Eligehausen, 1991.

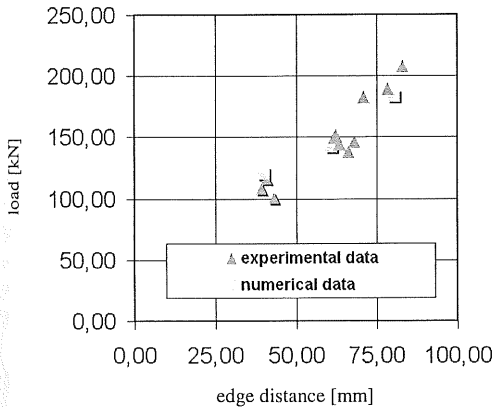


Figure 4. Influence of edge distance on failure load. Experimental results taken from Furche, Eligehausen, 1991.

Figure 4 shows a comparison between the ultimate loads measured in the experiments and obtained from the analysis. In all cases failure was caused by blow-out. The numerical results show a good agreement with the experimental results

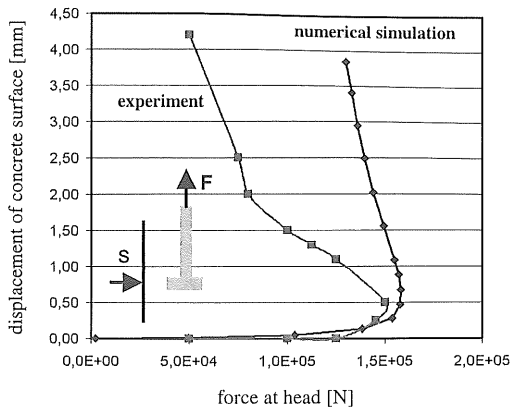


Figure 5. Displacement of concrete surface close to the head perpendicular to the surface. Test results are taken from Furche, Eligehausen, 1991.

In Figure 5 the lateral deformation of the concrete surface close to the head of the stud is plotted as a function of applied load. The numerical result agree sufficiently well with the experimental results. The lateral displacements increase fast after the maximum load is reached, indicating the failure of the concrete close to the head.

4 COMPARISON BETWEEN EXPERIMENTAL AND NUMERICAL RESULTS IN CASE OF EDGE FAILURE

4.1 Geometry and discretization

The geometry of the modeled structure is shown in Figure 6. A concrete slab with a height of 420 mm, a length of 740 mm and a width of $c + 270$ mm ($c =$ concrete cover) was modeled by eighth node solid elements. Between the steel elements of the headed stud and the concrete elements a contact layer with a thickness of 0.5 mm was placed. The material properties were adapted to the material properties obtained from the experimental investigations of Wüstholz (1999). The head stud was loaded in shear towards the edge. The supports were selected (Fig. 6) as in the experiment with a distance of four time the edge distance. In the analysis the available symmetry was used.

4.2 Numerical results and comparison with test results

A typical shear failure mode occurred in the numerical analysis as well as in the experiment. It is shown

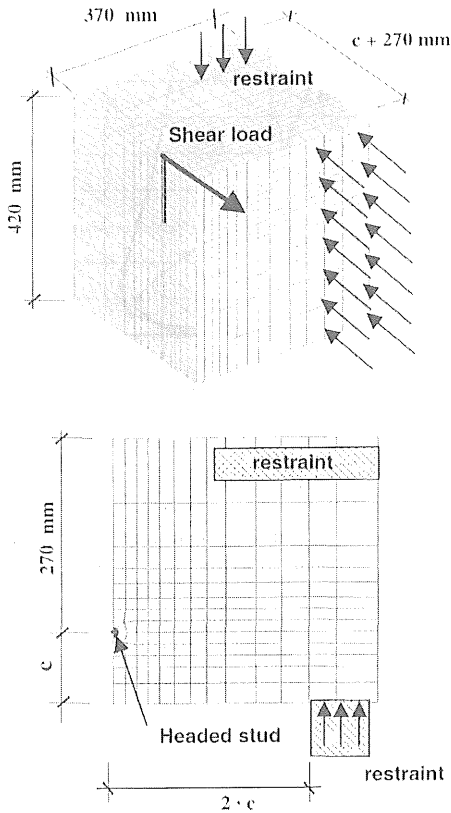


Figure 6. Geometry and finite element mesh of the test specimen loaded in shear towards the edge.

in Figures 7 and 8. The crack pattern obtained in the analysis shows a good agreement with the crack pattern observed in the test. The influence of the edge distance on the failure load is shown in Figure 9. For an edge distances of 60 mm and 100 mm a good agreement of the calculated maximum loads with the experimental data was reached. For an edge distance of 160 mm a local failure in front of the anchor occurred in the FE – simulation, which was not observed in the tests.

5 PARAMETRIC STUDY

5.1 Influence of the material parameters on tensile (blow out) resistance

The influence of the material parameters on the tensile load capacity of anchorages at the edge was examined. In each calculation only one parameter was varied, while the remaining parameters corresponded to the values of the reference model. In

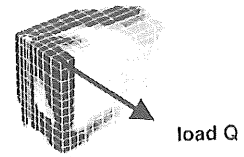


Figure 7. Post peak crack pattern ($h_{ef} = 130$ mm, $c = 100$ mm, shear load).

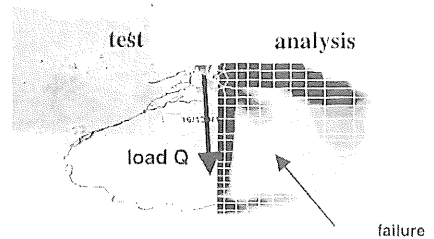


Figure 8. Post peak crack pattern ($h_{ef} = 130$ mm, $c = 100$ mm, shear load).

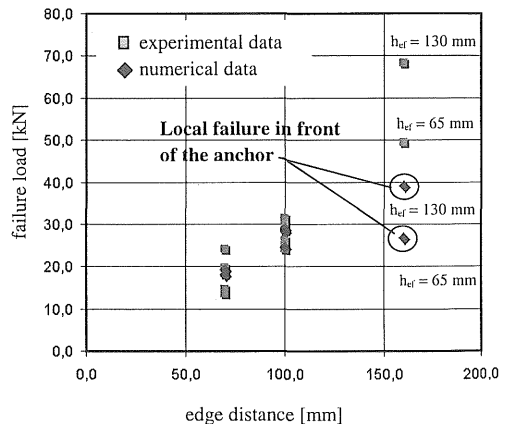


Figure 9. Influence of the edge distance on the failure load.

Figures 10a to 10d the calculated load displacement curves are shown. Varied was the concrete compression strength (Fig. 10a), the concrete tensile strength

(Fig. 10b), the fracture energy (Fig 10c) and the Young's modulus (Fig. 10d).

Figure 10a shows that the concrete compression strength f_c has a strong influence on the tension load capacity of a single anchor bolt at the edge. Increasing the concrete compression strength from 20 MPa to 30 MPa the tension load capacity increases by about 11 %, whereas an increase of the concrete compression strength from 30 MPa to 40 MPa causes an increase of the load capacity of 23 %. This increase in failure load with increasing concrete compression strength can be explained follow : Failure is caused by lateral bursting forces which are generated due to the high pressure ($10 \cdot f_c - 18 \cdot f_c$) under the anchor. With increasing the concrete compression strength a higher pressure under the head is needed to generate the same bursting force. The load displacement curves show that the behaviour becomes more brittle when the concrete compression strength increases.

According to Figure 10b the concrete tensile strength has also an influence on the tension load capacity. An increase of the concrete tensile strength from $f_t = 1.8$ MPa to $f_t = 2.8$ MPa causes an increase of the load capacity by about 18 %. A further increase to $f_t = 3.8$ MPa causes an increase of the tension load capacity of 6 % only. The load displacement behaviour does not change significantly.

The fracture energy G_f has an important influence on the maximum load and the load displacement behaviour. Figure 10c shows that a doubling of the fracture energy from $G_f = 0.05$ N/mm to $G_f = 0.10$ N/mm causes an increase of the failure load by 14 %. Doubling of the fracture energy from $G_f = 0.10$ N/mm to $G_f = 0.20$ N/mm gives an increase of 33 %. With the increase of the fracture energy G_f the behavior becomes more ductile.

The Young's modulus of concrete has a smaller influence on the failure load. In Figure 10d the load displacement curves with the Young's modulus of 20.000 MPa, 35.000 MPa and 40.000 MPa are plotted. They show that an increase of the Young's modulus causes an increases the tension load capacity by 4 % and 5 % respectively.

5.2 Influence of material properties on the shear concrete edge resistance

The influence of the material parameters on the shear loading capacity of anchorages at the edge is studied. In each calculation only one parameter was varied, while the remaining parameters corresponded to the values of the reference model. In Figures 11a to 11d the calculated load displacement curves are plotted. Varied was the concrete com-

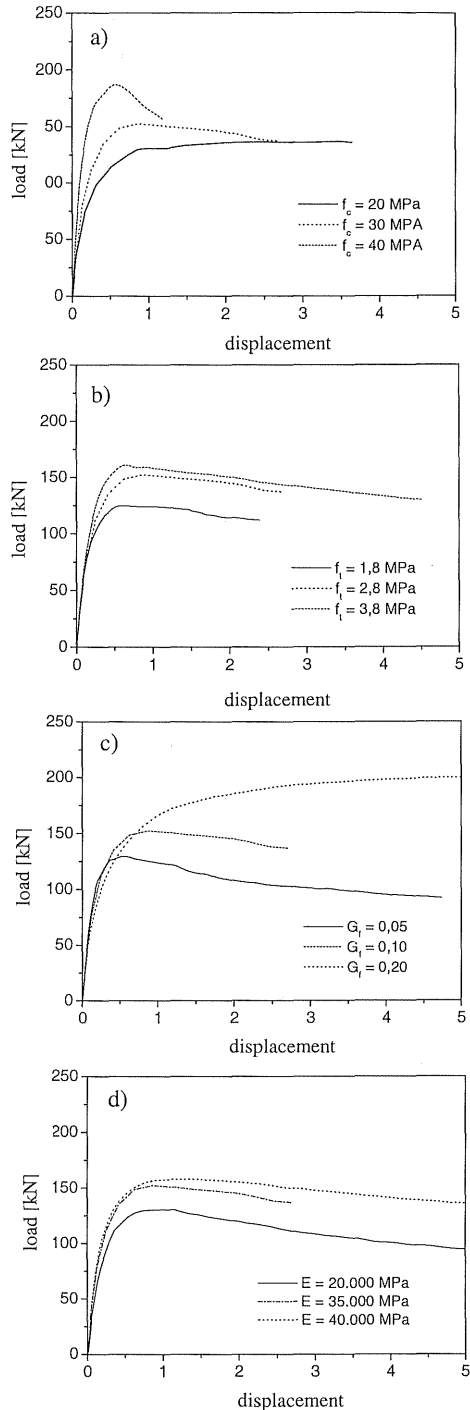


Figure 10. Calculated load - displacement curves showing the influence of the material properties : a) compression strength f_c , b) tensile strength f_t , c) fracture energy G_f and d) Young's modulus E .

pression strength (Fig. 11a), the concrete tensile strength (Fig. 11b), the fracture energy (Fig. 11c) and the Young's modulus (Fig. 11d).

Figures 10a shows that the concrete compression strength f_c has a visible influence on the shear load capacity of a single anchor bolt at the edge. Increasing the concrete compressive strength from 25 MPa to 35 MPa the shear load capacity increases by about 5 %, while a decrease of the concrete compressive strength from 25 MPa to 15 MPa causes a decrease of the shear load capacity of 10 %.

According to Figure 11b the concrete tensile strength has a strong influence on the shear load capacity. A decrease of the concrete tensile strength from $f_t = 2.5$ MPa to $f_t = 1.5$ MPa causes a decrease of the shear load capacity of about 13 %.

The fracture energy G_f has also an important influence on the maximum load and load displacement behavior. Figure 11c shows that an increase of the fracture energy from $G_f = 0.04$ N/mm to $G_f = 0.10$ N/mm causes an increase of the failure load by 14 %.

The Young's modulus of concrete exhibits a relatively strong influence on the shear load capacity. In Figure 11d the calculated load displacement curves with Young's modulus of 20.000 MPa, 30.000 MPa and 40.000 MPa are plotted. The figure show that an increase of the Young's modulus by 100 % increases the shear load capacity by 19 %.

The results of the parametric study are summarized in Figure 12. The figure shows that the failure load in the blow-out failure mode is more sensitive to the variation of the material properties than in the shear failure mode. With the blow-out failure mode the failure load increase approximately with $\psi^{0.4}$ ($\psi =$ parameter) (f_c , G_f) or $\psi^{0.25}$ (f_c , G_f).

On the contrary to that with the shear failure mode the increase is proportional to the varied parameter $\psi^{0.25}$.

6 CONCLUSION

The FE code MASA used in the present study is based on the microplane material model for concrete and on the smeared crack approach. As localization limiter the modified crack band method is used.

The comparison between the numerical and experimental data shows that the FE code is able to simulate the failure mechanism of headed stud anchorages placed close to edge under tensile loading or shear loading.

The parametric study indicates that failure load and the blow out failure mode is more sensitive to the variation of material properties than in the shear failure mode.

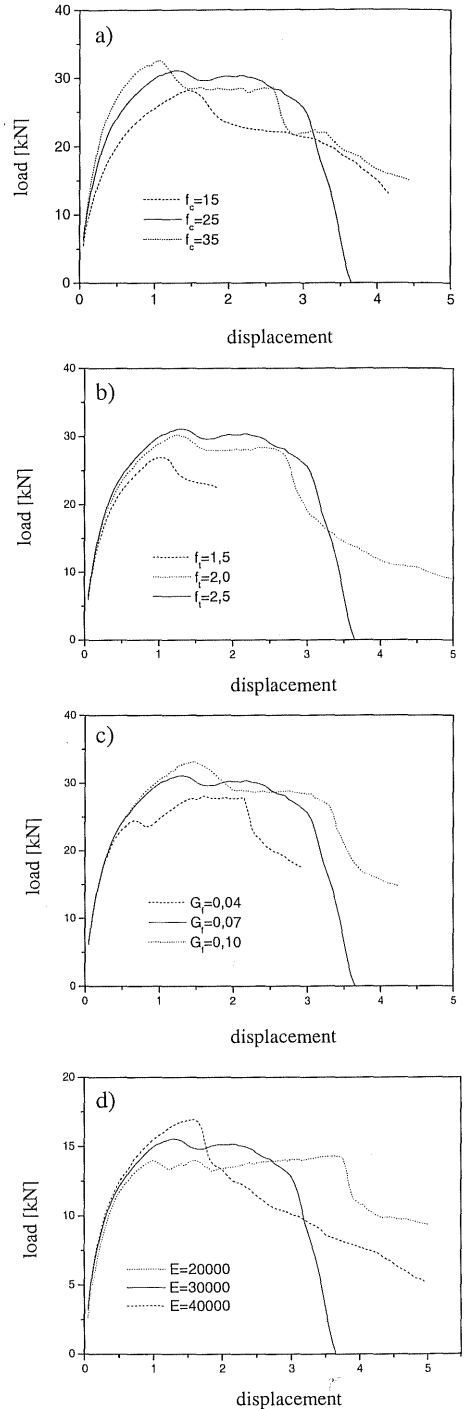


Figure 11. Calculated load - displacement curves of the reference model showing the influence of the material properties : a) compression strength f_c , b) tensile strength f_t , c) fracture energy G_f and d) Young's modulus E .

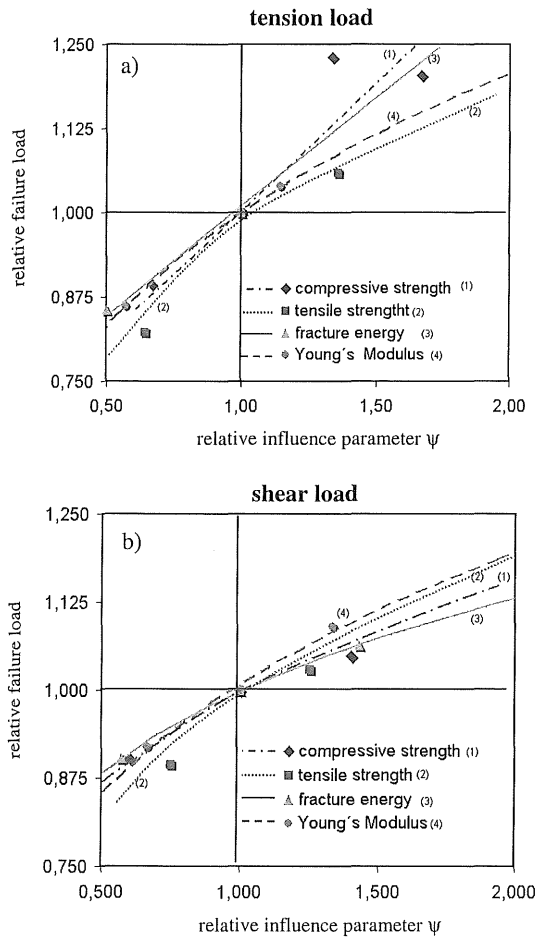


Figure 12. Comparison of the relative influence of material properties of headed studs under a) tension load. and b) shear.

7 REFERENCES

- Ožbolt, J.; Li, Y.-J. and Kožar, I. (2001). Microplane model for concrete with relaxed kinematic constraint. *International Journal of Solids and Structures*, in press.
- Fuchs, W.; Eligehausen, R and Breen, J.E. (1995). Concrete Capacity Design (CCD) Approach for Fastenings to Concrete. *ACI Structural Journal*, Vol. 92, No. 6, S794-802
- FEMAP (1997) – Finite Element Modelling and Postprocessing, Ver. 5.00a, Copyright © Enterprise Software Products, Inc.
- Furche J.; Eligehausen, R. (1991). Lateral Blouout Failure of headed Studs Near the Free Edge. In: Senkiw, G.A. ; Lancelot, H.B., SP-130 Design an Behavior . American Concrete Institute, Detroit, page 235 – 252.
- Wüstholz, T (1999). Tragverhalten von randnahen Befestigungsmitteln unter Querlasten bei der Versagensart Beton-